

DEUTSCHES ELEKTRONEN-SYNCHROTRON
Ein Forschungszentrum der Helmholtz-Gemeinschaft

DESY 13-162

September 2013

**Nonlinear undulator tapering in conventional
SASE regime at baseline electron beam
parameters as a way to optimize the radiation
characteristics of the European XFEL**

Svitozar Serkez^a, Vitali Kocharyan^a, Evgeni Saldin^a, Igor
Zagorodnov^a and Gianluca Geloni^b

^a*Deutsches Elektronen-Synchrotron DESY, Hamburg*

^b*European XFEL GmbH, Hamburg*

ISSN 0418-9833

NOTKESTRASSE 85 - 22607 HAMBURG

Nonlinear undulator tapering in conventional SASE regime at baseline electron beam parameters as a way to optimize the radiation characteristics of the European XFEL

Svitozar Serkez ,^{a,1} Vitali Kocharyan,^a Evgeni Saldin,^a
Igor Zagorodnov,^a and Gianluca Geloni^b

^a*Deutsches Elektronen-Synchrotron (DESY), Hamburg, Germany*

^b*European XFEL GmbH, Hamburg, Germany*

Abstract

We demonstrate that the output radiation characteristics of the European XFEL sources at nominal operation point can be easily made significantly better than what is currently reported in the TDRs of scientific instruments and X-ray optics. In fact, the output SASE characteristics of the baseline European XFEL have been previously optimized assuming uniform undulators at a nominal operating point of 5 kA peak current, without considering the potential of undulator tapering in the SASE regime. In order to illustrate this point, we analyze the case of an electron bunch with nominal parameters. Based on start-to-end simulations, we demonstrate that nonlinear undulator tapering allows one to achieve up to a tenfold increase in peak power and photon spectral density in the conventional SASE regime, without modification to the baseline design. The FEL code Genesis has been extensively used for these studies. In order to increase our confidence in simulation results, we cross-checked outcomes by reproducing simulations in the deep nonlinear SASE regime with tapered undulator using the code ALICE.

1 Introduction

The technical note [1] provides an overview of the design considerations and the general layout of the X-ray instrumentation of the European XFEL sources, beam transport systems and instruments. Baseline parameters for

¹ Corresponding Author. E-mail address: svitozar.serkez@desy.de

the electron beam have been defined and presented in [2]. These parameters have been used for simulating FEL radiation characteristics and saturation lengths relevant to the European XFEL SASE undulators [3]. The definition of saturation point used throughout [1] is reported here: "Saturation is reached at the magnetic length at which the FEL radiation attains maximum brilliance. Beyond the saturation point, the FEL operates in an over saturated mode where more energy can be extracted from the electron beam at the expense of FEL parameters, including bandwidth, coherence time, and degree of transverse coherence".

An approach based on the exploitation of the baseline electron beam characteristics in [2], together with the definition of the saturation point reported above and with the notion that the best FEL parameters are found at saturation has been quite useful as a convenient starting point for the analysis of XFEL sources, beam transport systems and instruments. However, based on recent advancement in the FEL field, here we argue that there are two main reasons why such approach should be modified.

First, the above-mentioned approach is based on the baseline parameters for the electron beam [2] assuming an operation point at 5 kA peak current. This choice is subjective. There is a possibility to go well beyond the nominal peak current level. For example, in order to illustrate the potential of the European XFEL accelerator complex, in [4] considerations were focused on an electron bunch with 0.25 nC charge, compressed up to a peak current of about 50 kA. An advantage of operating at such peak current is the increase of the X-ray output peak power without of any modification to the baseline design [5]. The price for using a very high peak current is a large energy chirp within the electron bunch, yielding in turn a large (about 1%) SASE radiation bandwidth. However, there are very important applications like bio-imaging, where such extra-pink X-ray beam is sufficiently monochromatic to be used as a source for experiments without further monochromatization. The example presented in [5] demonstrates that there is no universal choice of baseline electron beam parameters: such choice should be considered, at least, as dependent on the instruments.

Second, the analysis presented in [1] is based on the use of uniform undulators only. A fundamental example showing the limitations of such model for the analysis of the European XFEL is constituted by undulator tapering effects. In fact, one obvious way to enhance the SASE efficiency is by properly configuring undulators with variable gap [6]-[15].

Abandoning the assumption of uniform undulators alone has far reaching consequences. Here we illustrate the potential of undulator tapering in the SASE regime by still considering an electron bunch with the usual baseline parameters [2], i.e. the same assumed in [1], and in all the subsequent TDR.

A significant increase in power is achievable by nonlinear rather than linear undulator tapering [15]. In particular, in this article we will demonstrate that nonlinear undulator tapering allows one to achieve up to a tenfold increase not only in peak power but also in photon spectral density of the output radiation pulses. In order to illustrate this point we will make an analysis for the baseline (21 cells) SASE3 undulator at the nominal electron beam energy 14 GeV. We first optimize our setup based on start-to-end simulations for the electron beam with 0.1 nC, compressed up to 5 kA peak current [2]. In this way, the SASE saturation power in the uniform undulator could be as large as 60 GW. Subsequently, in order to generate high-power X-ray pulses we exploit undulator tapering. Tapering consists in a slow reduction of the field strength of the undulator in order to preserve the resonance wavelength, while the kinetic energy of the electrons decreases due to the FEL process. The undulator taper can be simply implemented as discrete steps from one undulator segment to the next, by changing the undulator gap. In this way, the output power of the SASE3 undulator could be increased from the value of 60 GW in the SASE saturation regime to about 750 GW. One might be surprised that the photon spectral density increases of about a factor ten as well (see section 2 for more details).

The analysis of the nonlinear FEL process refers to a problem that can be solved only numerically. The Genesis code [16] has been extensively used for our FEL studies. However, an accurate simulation of the deep nonlinear SASE regime in a tapered undulator remains a challenging problem for numerical analysis. During the last decade, several additional FEL codes have been developed around the world. In order to increase our confidence in the simulation results, we cross-checked them with one of these, the code ALICE [17].

Summing up, in this article we demonstrate that the performance of European XFEL sources can be significantly improved without additional hardware. The optimization procedure simply consists in the optimization of the undulator gap configuration for each X-ray beamline. Based on these findings, we suggest that new baseline radiation parameters be defined, and that the requirements for the instruments and beam transport systems be updated.

2 FEL studies

As described in the Introduction, in this paper we focus our attention on the tremendous increase in SASE efficiency that can be achieved using a tapering undulator technique. It must be stressed that in actual studies we let aside our remark concerning the optimization of the electron beam

Table 1

Parameters for the mode of operation at the European XFEL used in this paper.

	Units	
Undulator period	mm	68
Periods per cell	-	73
Total number of cells	-	21
Intersection length	m	1.1
Energy	GeV	14
Charge	nC	0.1

nominal working point, and we proceed in the analysis of the benefits deriving from the application of tapering for the baseline (21 cells) SASE3 undulator at the nominal electron beam energy of 14 GeV, considering a 0.1 nC bunch, compressed up to 5 kA peak current [2]. The main electron and undulator parameters for simulations are shown in Table 1.

The nominal electron beam characteristics resulting from start-to-end simulations are shown in Fig. 1 in terms of current, emittance, energy spread and energy. In addition, Fig. 1 also shows the resistive wake in the SASE3 undulator. Additional energy chirp introduced by resistive wakes in the SASE1 undulator vacuum chamber are included in our simulations, as well as quantum diffusion effects.

In this Section we show how proper undulator tapering allows one to increase the peak radiation power of the European XFEL SASE sources from the 100 GW power-level up to the TW power-level. In order to perform the undulator tapering optimization we followed the theoretical work done at DESY [13] and SLAC [15], which was used for self-seeded tapered XFELs, showing that the baseline undulator greatly benefit of this treatment as well. To be specific, we used the taper profile in [15]

$$\begin{aligned}
 K(z) &= K(z_0) , & \text{when } 0 < z < z_0 , \\
 K(z) &= [K(z_0) + d] \cdot [1 - a(z - z_0)^b] , & \text{when } z_0 < z < L_w ,
 \end{aligned}
 \tag{1}$$

where K is undulator parameter, z_0 indicates the taper starting point, b is the taper profile order, a is a scale coefficient, and d is the change in undulator parameter at the tapering start point location. Empirically, the best taper starting point was found to be located slightly before the initial saturation point, and the taper profile order is around $b \simeq 1.5$. This specification for the functional dependencies of the undulator parameter allowed us to obtain the maximum radiation power for the tapered FEL with baseline electron beam described above by performing multidimensional scans with Genesis

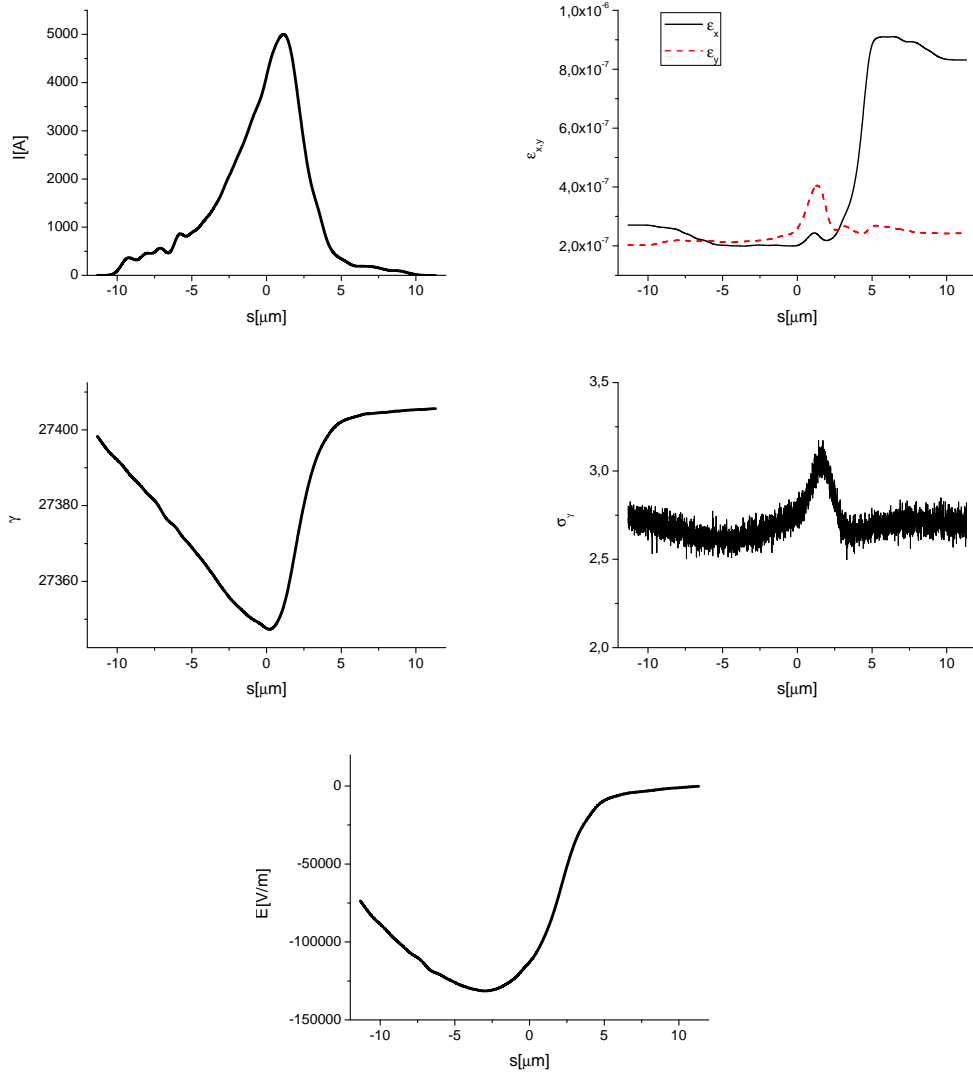


Fig. 1. Results from electron beam start-to-end simulations at the entrance of SASE3. (First Row, Left) Current profile. (First Row, Right) Normalized emittance as a function of the position inside the electron beam. (Second Row, Left) Energy profile along the beam. (Second Row, Right) Electron beam energy spread profile. (Bottom row) Resistive wakefields in the SASE3 undulator.

SASE simulations over the following four parameters z_0 , a , b , and d . Such optimization resulted in the tapering law graphically shown in Fig. 2, for radiation emitted at 2 keV. Additionally, as originally proposed in [15], we assumed a linear change, along the undulator longitudinal coordinate z , in the strength of the quadrupole field, Fig. 3 (left) leading to the evolution of the electron bunch transverse dimensions shown in Fig. 3 (right).

All simulations were performed using the code Genesis 1.3 [16] running on a parallel machine. Results are presented for the SASE3 FEL line of the European XFEL, based on a statistical analysis consisting of 100 runs, and

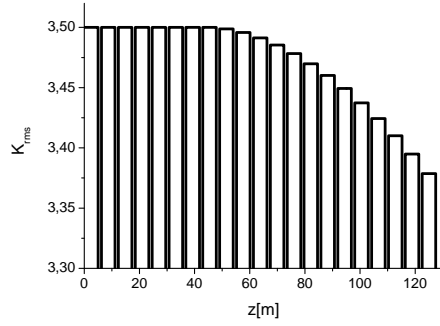


Fig. 2. Taper configuration for high-power mode of operation at 0.6 nm.

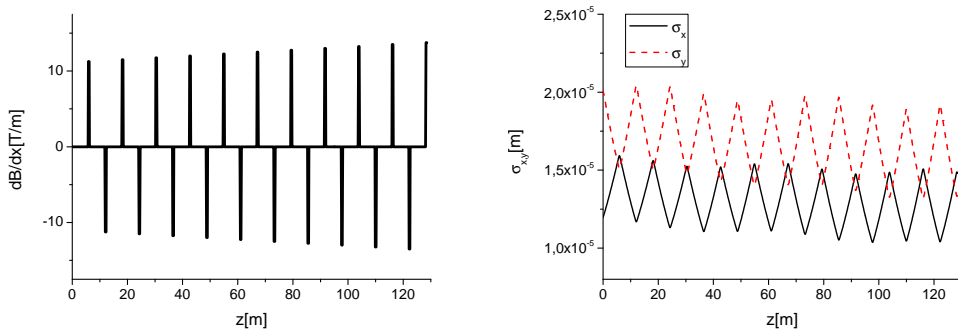


Fig. 3. Left plot: linear increase in the magnetic field quadrupole gradient assumed in this paper. Left plot: consequent evolution of the horizontal and vertical dimensions of the electron bunch as a function of the distance inside the SASE3 undulator. The plot refers to the longitudinal position inside the bunch corresponding to the maximum current value.

comparing the SASE regime at saturation with the tapered SASE regime.

Fig. 4 shows a comparison of power and spectrum produced in the standard SASE mode at saturation (and, therefore, without tapering) and power and spectrum produced in the standard SASE mode including post-saturation tapering. What is important to notice here, is that a tenfold increase in the shot-to-shot averaged spectral energy density can be seen by inspection. Fig. 5 shows the evolution of the output energy in the photon pulse and of the variance of the energy fluctuation as a function of the distance inside the output undulator, including tapering.

Finally, in Fig. 6 we show a comparison of radiation beam size and divergences for the SASE operation mode in saturation, and for the tapered SASE mode. If one considers, as an example, the case when pink light is delivered to the Small Quantum Systems (SQS) station, the only optics encountered by the SASE3 beam transport line is a pair of horizontal offset mirrors. This mirror system can be adjusted between 6 mrad and 20 mrad incidence angle. After the offset is introduced, the beam can be directly transported to the

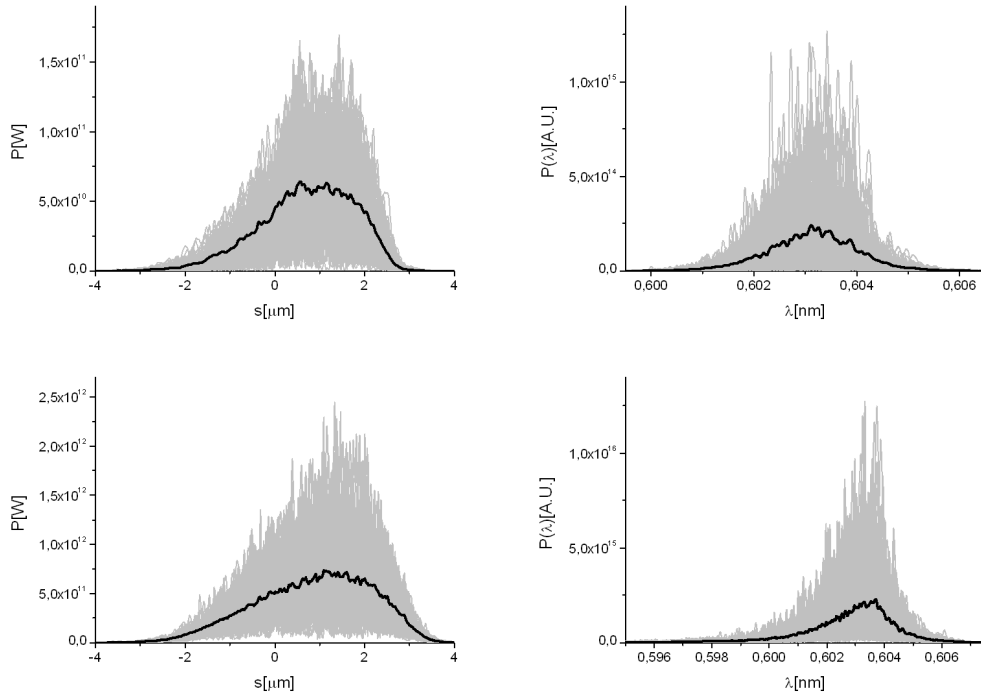


Fig. 4. Top row: Power and spectrum produced in the standard SASE mode at saturation (and, therefore, without tapering). Bottom row: Power and spectrum produced in the standard SASE mode including post-saturation tapering. Scales of spectral energy density are the same for both cases. Grey lines refer to single shot realizations, the black line refers to the average over a hundred realizations. A tenfold increase in the shot-to-shot averaged spectral energy density can be seen by inspection.

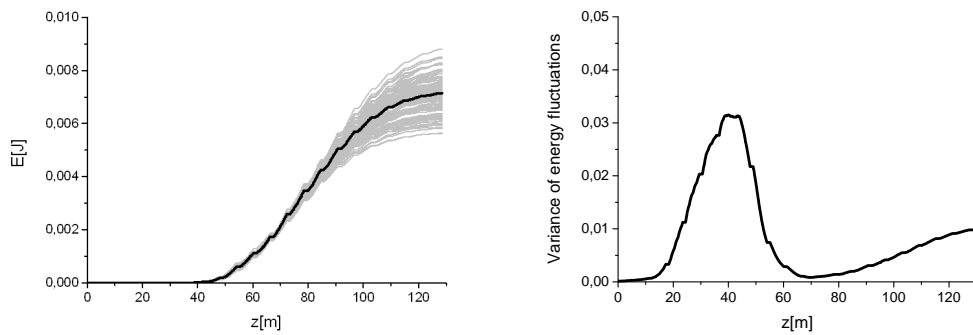


Fig. 5. Evolution of the output energy in the photon pulse and of the variance of the energy fluctuation as a function of the distance inside the output undulator, with tapering. Grey lines refer to single shot realizations, the black line refers to the average over a hundred realizations.

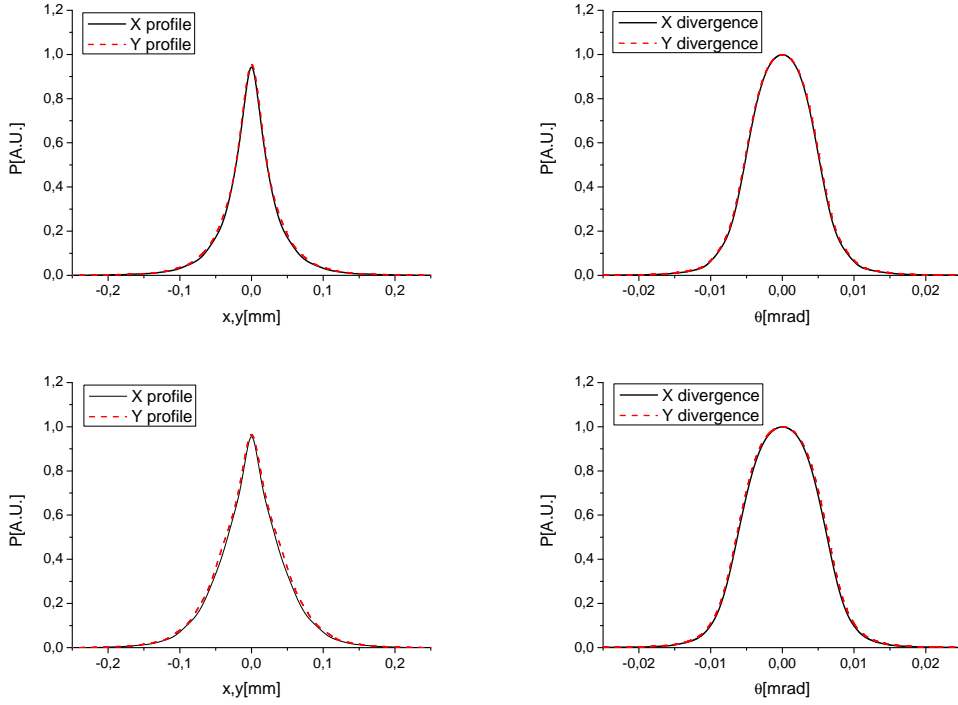


Fig. 6. Top row: Distribution of the radiation pulse energy per unit surface and angular distribution at saturation. Bottom row: Distribution of the radiation pulse energy per unit surface and angular distribution at the exit of the setup.

SQS instrument [18]. The offset mirrors are placed about 300 m behind the source point. Since one needs to minimize diffraction from the optics aperture and to preserve the radiation wavefront, any optical element should ideally have an aperture size large enough to accept at least 4σ times the beam size. In our simulation study, the FWHM divergence of the FEL beam in the tapered undulator case is of the order of $12 \mu\text{rad}$ at 2 keV (see Fig. 6). Therefore, the lateral aperture of the radiation at the offset mirrors position turns out to be about 6 mm (or 3.6 mm FWHM) for our case of interest.

The lateral aperture of the radiation which is accepted by the mirror is limited by the grazing angle and the length of the mirror. More specifically, we can estimate the transverse clear aperture of a grazing-incidence mirror as $L\theta$, L being the mirror clear aperture, and θ being the grazing incidence angle. The X-ray optics and transport group is planning to implement offset mirrors with a clear aperture of 800 mm (see e.g. [19]). With 9 mrad reflection angle we obtain a transverse clear aperture of 7.2 mm, which is in principle enough to fulfill the 4σ requirement.

Finally, the transmission for the pair of offset mirrors for 9 mrad incidence angle calculated, for B4C coating is about 90% at a photon energy of 2 keV [19].

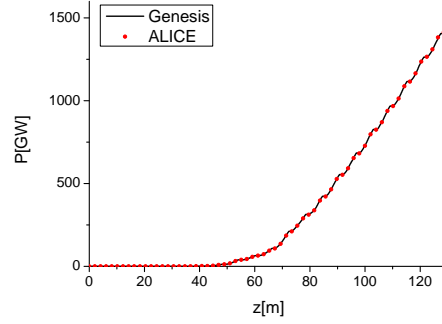


Fig. 7. Comparison between Genesis and ALICE predictions for the output power as a function of the position inside the undulator in the steady state regime. The FEL configuration considered here refer to the SASE3 undulator line operating at 14 GeV. The photon energy chosen for the comparison is 2 keV. Electron beam characteristics refer to the longitudinal position, inside the 0.1 nC bunch, corresponding to the maximum current value. The undulator magnetic field file corresponds to the optimum for the SASE tapering regime (see above in this section)

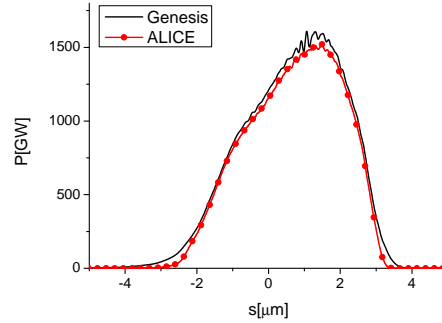


Fig. 8. Comparison between Genesis and ALICE predictions for the output power as a function of the position inside the electron bunch in time-dependent case for seeded FEL amplifier regime, including tapering. The FEL configuration considered here refer to the SASE3 undulator line operating at 14 GeV. The photon energy chosen for the comparison is 2 keV. Input electron beam and undulator magnetic files are the same as in Fig. 4, bottom row.

3 Cross-checking of Genesis simulations

While the code Genesis has had an undiscussed success to reproduce results from LCLS experiments and has been thoroughly benchmarked, next generation FEL codes like ALICE [17] recently began to appear, which take advantage of more and more advanced algorithms. In ALICE, the equations of motion for the particles are integrated with a symplectic “leap-frog” scheme. The parabolic field equation is solved with the help of an implicit Neumann finite difference scheme, based on azimuthal expansion. Additionally, open boundary conditions with the help of the Perfectly Matched

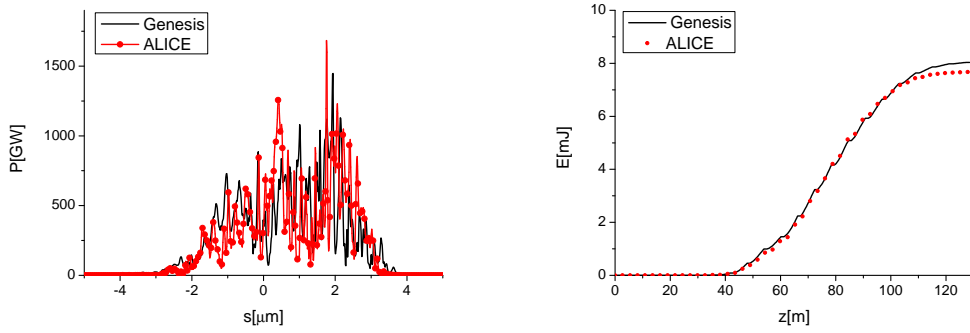


Fig. 9. Comparison between Genesis and ALICE predictions in the time-dependent case for SASE regime, including tapering. The FEL configuration considered here refer to the SASE3 undulator line operating at 14 GeV. The photon energy chosen for the comparison is 2 keV. Left plot: output power for a typical single shot. Right plot: energy per pulse. Since codes are not identical, SASE initial conditions are not the same, and we can expect some difference within results. Because of this reason, codes can be considered in very good agreement.

Layer (PML) method for parabolic equations were implemented. The code is parallelized and allows one to use full three dimensional models for both the electron beam and the radiation field.

In order to increase the confidence in our simulation results, we cross-checked them with ALICE. In Fig. 7, Fig. 8 and Fig. 9 we show comparisons of simulations obtained with these two codes, for undulator configurations similar to those considered in this section. The agreement in the steady state regime and in the time-dependent seeded FEL amplifier regime is perfect. In the SASE regime the agreement is reasonably good. Despite the simulation of deep nonlinear SASE regime is the challenging problem for numerical analysis and codes adopted different numerical methods, the pulse energy differs by only 10%. Differences in the output are well within an rms of shot-to-shot fluctuations (see Fig. 9). The SASE process is driven by the intrinsic shot noise in the electron beam current, and a random generator is used in each code to fill-in the initial particle distribution. Therefore, differences in the SASE regime are ascribed to different initial SASE signals.

4 Conclusions

In this article we demonstrated that the output characteristics of the European XFEL in SASE mode can be substantially improved, without any additional hardware installation. At variance with previous numerical studies for the European XFEL, in this work we included energy chirp, wakefields and undulator tapering effects for a segmented undulator with intersections,

and we assumed realistic distributions for the electron beam current, for the energy spread and for the emittance in the horizontal and vertical direction along the bunch. The importance of realistic models in XFEL simulations is amply demonstrated in this paper. In order to take into consideration wake-field effects and to examine the impact of undulator tapering on radiation properties, electron bunches are treated on the basis of start-to-end simulations and the undulator includes intersections with phase shifters. In order to obtain optimal performance, both undulator gap and phase shifters had to be tuned. It has been shown that the taper provides an additional factor of ten increase in spectral density and output power (up to the TW-level) for a baseline electron beam parameter set. We anticipate that, mainly by increasing the peak current of the driving electron beam beyond the baseline value of 5 kA it will be possible to achieve a further increase of x-ray power beyond the TW-level. The European XFEL uses a superconducting L-band linac to accelerate electron beams, which can be compressed up to extremely high peak currents of about 50 kA, with still a reasonable electron bunch quality [4]. The maximal electron beam energy at the European XFEL is 17.5 GeV. It is worthwhile to mention that 50 kA peak current at 20 GeV beam energy corresponds to 1 PW peak power of electron beam. In [5] we demonstrated that with a PW power level of driving electron beam and a long enough, high K-value undulator it would be possible to achieve a 10 TW-level X-ray beam at the European XFEL without additional hardware. For a long time, such unique feature will be available only at the European XFEL.

5 Acknowledgements

We are grateful to Massimo Altarelli, Reinhard Brinkmann, Henry Chapman, Janos Hajdu, Viktor Lamzin, Serguei Molodtsov and Edgar Weckert for their support and their interest during the compilation of this work.

References

- [1] Th. Tschentscher, "Layout of the x-Ray Systems at the European XFEL", Technical Report 10.3204/XFEL.EU/TR-2011-001 (2011).
- [2] I. Zagorodnov, "Beam Dynamics Simulations for XFEL", <http://www.desy.de/xfel-beam/s2e> (2011).
- [3] E. Schneidmiller and M. Yurkov, Photon beam properties at the European XFEL, DESY 11-152 (2011) (and updates).
- [4] I. Zagorodnov, "Compression scenarios for

- the European XFEL", http://www.desy.de/fel-beam/data/talks/files/Zagorodnov_ACC2012_ready_new.pptx, (2012).
- [5] S. Serkez et al., "Proposal to generate 10 TW level femtosecond x-ray pulses from a baseline undulator in conventional SASE regime at the European XFEL", DESY 13-138 (2013).
 - [6] A. Lin and J.M. Dawson, Phys. Rev. Lett. 42 2172 (1986).
 - [7] P. Sprangle, C.M. Tang and W.M. Manheimer, Phys. Rev. Lett. 43 1932 (1979).
 - [8] N.M. Kroll, P. Morton and M.N. Rosenbluth, IEEE J. Quantum Electron., QE-17, 1436 (1981).
 - [9] T.J. Orzechowski et al., Phys. Rev. Lett. 57, 2172 (1986).
 - [10] W. Fawley et al., NIM A 483 p 537 (2002).
 - [11] M. Cornacchia et al., J. Synchrotron rad. 11, 227-238 (2004).
 - [12] X. Wang et al., PRL 103, 154801 (2009).
 - [13] G. Geloni, V. Kocharyan and E. Saldin, "Scheme for generation of fully coherent, TW power level hard x-ray pulses from baseline undulators at the European XFEL", DESY 10-108 (2010).
 - [14] W.M. Fawley et al., Toward TW-level LCLS radiation pulses, TUOA4, FEL 2011 Conference proceedings, Shanghai, China (2011).
 - [15] Y. Jiao et al. Phys. Rev. ST Accel. Beams 15, 050704 (2012).
 - [16] S. Reiche et al., Nucl. Instr. and Meth. A 429, 243 (1999).
 - [17] I. Zagorodnov and M. Dohlus, Proceedings of FEL 2009 MOPC16 (2009), I. Zagorodnov, Proceedings of ICAP 2012 TUACI1 (2012).
 - [18] T. Mazza, H. Zhang and M. Meyer, Scientific Instrument SQS Technical Design Report, XFEL.EU TR-2012-007 (2012).
 - [19] H. Sinn et al., X-Ray Optics and Beam Transport Technical Design Report, XFEL.EU TR-2012-006 (2012).